

CORROSION FATIGUE FRACTURE BEHAVIOR OF HIGH-STRENGTH Cu TROLLEY WIRE FOR HIGH-SPEED RAILROAD SERVICES

K. Minoshima, K. Miyazawa and K. Komai

Department of Mechanical Engineering, Kyoto University, Kyoto 606-8501, Japan

ABSTRACT

One of the limiting factors in an operation of a high-speed train is the wave propagation rate in trolley wire, because the current collecting performance is reduced when the speed of a train reaches the wave propagation rate. Therefore, an operation of a high-speed train requires trolley wire with high wave propagation rates. For this purpose, the trolley wire should be tightened up with high tension stress which in turn requires a high-strength property and/or should have less density, although the mechanical properties including wear and (corrosion) fatigue and other properties such as electric properties should be sufficient. In this investigation, fatigue and corrosion fatigue properties have been evaluated in a newly developed high-strength Cu-Sn trolley wire for an operation of a high-speed train. The influence of NaCl solution on corrosion fatigue life is negligible, because of relief of stress concentration due to initiation of multiple cracks, blunting of corrosion fatigue crack tip by dissolution, and decrease in total crack depth due to general corrosion on the wire. Therefore, the corrosion fatigue strength is determined by mechanical fatigue strength in air. Attention is also paid to crack initiation and corrosion behavior by using scanning electron and atomic force microscopy, and the mechanisms of corrosion fatigue are discussed.

KEYWORDS

Corrosion fatigue, Crack initiation, Atomic force microscopy, Trolley wire for High-Speed Railroad Services

INTRODUCTION

Continuous progress in science and technology creates increasing demands for further improved materials. The material degradation phenomenon, corrosion fatigue, is one of the most important issues for machine and structural design when the material is subjected to varying loads and a corrosive environment. One of the important processes of corrosion fatigue is that a crack is nucleated at a corrosion pit formed on the surface, and then it propagates to final failure. Some investigations into the mechanical condition of the crack initiation at a corrosion pit were already reported [1–3]. In order to analyze the initiation and propagation process of a corrosion fatigue crack, scanning electron microscopy is widely used, which has fascinating characteristics: i) a broad band of magnifications easily facilitates the correlation of macroscopic and microscopic images; ii) a high depth of field or focus is attained, and a rough surface such as a fracture surface is clearly imaged in a three-dimensional or panoramic manner. However, a drawback is that it is only capable of imaging in vacuum, and therefore serial, *in situ* imaging of a corrosion or crack initiation process is impossible, and that the vertical resolution is low for observing the very early stage of surface damage. In contrast with these, an atomic force microscope is capable of imaging the surface not only in vacuum, but also in air or in liquid, and thereby *in situ* high-magnification imaging is possible. Up to dates, it is applied to *in situ* observation of a growth process of a stress corrosion crack [6, 7], early fatigue crack initiation stage of a metal [8–10] and so on.

On one hand, speedup of railroad transportation of both Shinkansen lines and conventional lines is planned by Japanese railroad companies. In order to realize a high-speed electric train service, wave propagation velocity in the trolley wire must be increased. This is because when the train speed approaches the wave propagation velocity, the current-collecting performance is decreased owing to multi-pantograph induced resonance and uplift of the contact wire. Therefore, the maximum speed of the trains is limited to about 70% of the wave

propagation velocity. In order to increase the wave propagation velocity, two measures are utilized: one is to decrease the density of the trolley wire and the other is to increase the wiring tension. To increase the wiring tension, the strength of the trolley wire must be high enough for such high-tension during service. However, high-strength metallic materials are usually sensitive to stress corrosion cracking and corrosion fatigue, and therefore, the influence of environment on the strength must be clarified.

In this investigation, the fatigue tests in air and in a 3.5% NaCl solution were conducted in a newly developed high-strength Cu trolley wire for Shinkansen lines. In particular, the surface damage initiation and propagation were closely examined by a scanning electron microscope and an atomic force microscope, and the mechanisms of corrosion fatigue of the high-strength Cu trolley wire were discussed.

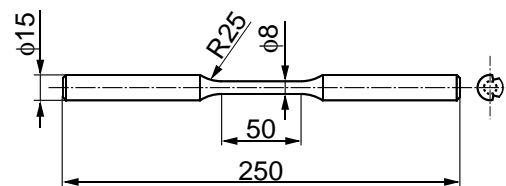


Figure 1: Shape and dimensions of smooth test specimens. All dimensions are in mm.

EXPERIMENTAL PROCEDURES

The material used was a newly developed Cu-trolley wire (Cu-0.36% Sn (O: 410 ppm, Ag: 8 ppm, other impurities (Fe, Co, Pb, Bi, Ni, Sb, As, and Te) less than 1 ppm), in mass). To achieve as much conductivity as that of the conventional Cu trolley wire and to increase the strength, the amount of Sn and the working are increased. This enables the high wiring tension of 19.6 kN for 160 mm²-trolley wire, where the wave propagation velocity is about 410 km/h (\approx 114 m/s). The smooth round specimens shown in Fig. 1 were machined from the actual trolley wire. For the fatigue tests conducted at a lower stress, the specimen diameter of 6 mm is adopted to avoid fretting fatigue failure at a gripping position. The middle part of a sample was ground to #1500 by wet emery paper, and then finished by 1 μ m diamond paste. In a corrosive environment, the middle part of 20 mm in gage length was exposed to an environment, and others were anti-corrosive coated. The corrosive environment was a 3.5% NaCl solution prepared by reagent grade NaCl and ion-exchanged water whose relative resistance was larger than 1 M Ω ·cm. The solution, which was kept at 298 \pm 1 K, was circulated by a vane pump between a corrosion reservoir and a environmental cell attached to the specimen. The amount of the solution circulated was 10 L, and 3 L solution was exchanged every three days.

The testing machine employed was a computer-controlled, electro-hydraulic fatigue testing machine (Loading capacity: 98 kN). The tensile tests were conducted under displacement control: the displacement rate was 1 mm/min in laboratory air and 0.005 mm/min in a NaCl solution. Fatigue tests were conducted at a stress cycle frequency of 20 Hz with sinusoidal stress wave form. The tests were conducted at a constant mean stress of 115 MPa. This is because the trolley wire is used under tension of 19.6 kN, which gives the tensile stress of 115 MPa (cross sectional area: 170 mm²). Two types of fatigue tests were conducted: one was to run the fatigue tests to final failure, and the other was an interrupted test, where the test was periodically interrupted and the surface damage was observed, until the specimen failed. When observing the specimen surface, the surface was ultrasonically cleaned in ethyl alcohol followed by in deionized water.

The specimen surface was observed by a scanning electron microscope. Some were closely examined by using an atomic force microscope (NanoScope IIIa and Dimension 3000 system, Digital Instruments, Ltd., USA), which has a large sample stage, and thereby the specimen surface was examined without cutting.

EXPERIMENTAL RESULTS AND DISCUSSIONS

Tensile Strength and Fracture Morphology

Table 1 summarizes the results of tensile tests conducted in laboratory air and in NaCl solution. The tensile strength obtained under a low strain rate in NaCl solution, (a slow strain rate test: SSRT), was the same as that conducted in laboratory air. The fracture in NaCl solution occurred in a cup-and-cone manner, similarly to the case of tensile tests in laboratory air. The microscopic fracture was dominated by dimples both in laboratory air and in NaCl solution. These indicate that the fracture occurred in a ductile manner in both environments, and the susceptibility to stress corrosion in a 3.5% NaCl solution is considered low.

Fatigue Fracture Behavior

Corrosion fatigue strength

Figure 2 illustrates the relationship between the stress amplitude and the number of cycles to failure (S-N

TABLE 1
Mechanical properties of Cu trolley wire in laboratory air and in 3.5% NaCl solution.

	Tensile Strength	Elastic Modulus	Elongation at Break
Laboratory air	473 MPa	125 GPa	8%
3.5% NaCl soln	482 MPa	122 GPa	6%

Displacement rate: 1 mm/min (Laboratory air)
0.005 mm/min (NaCl solution)

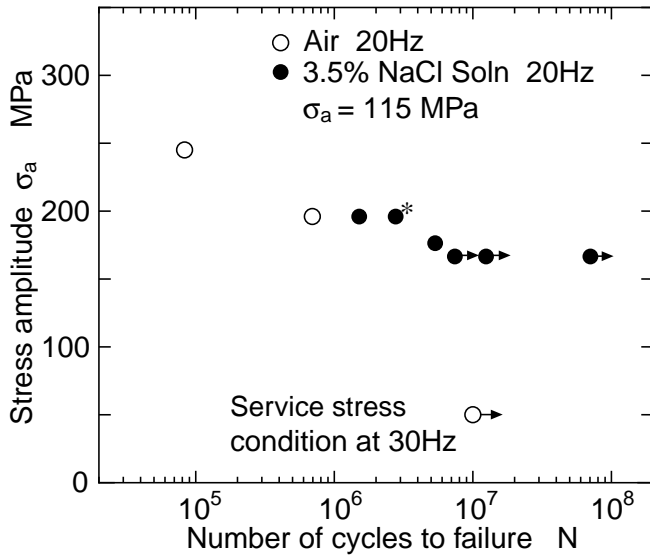
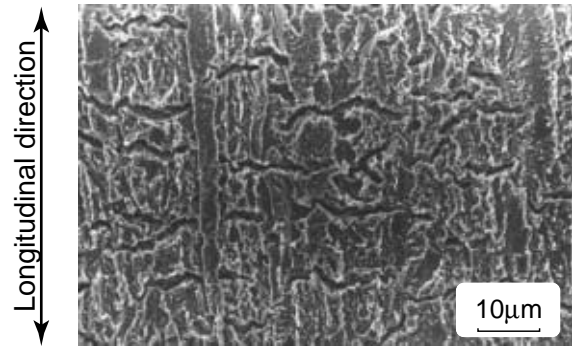
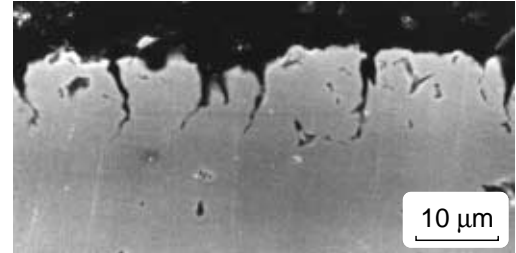


Figure 2: S-N curves of Cu trolley wire in laboratory air and in a 3.5% NaCl solution at 25°C. The tests were conducted under a mean stress of 115 MPa, corresponding to tension stress of the trolley wire in a service condition.



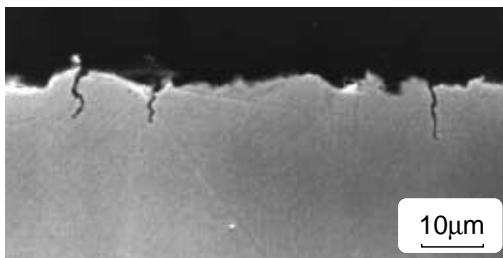
(a) Sample surface.



(b) Cross section along the longitudinal direction
Figure 3: Corrosion fatigue damage at $\sigma_a = 196$ MPa ($\sigma_m = 115$ MPa, $N_f = 1.5 \times 10^6$)

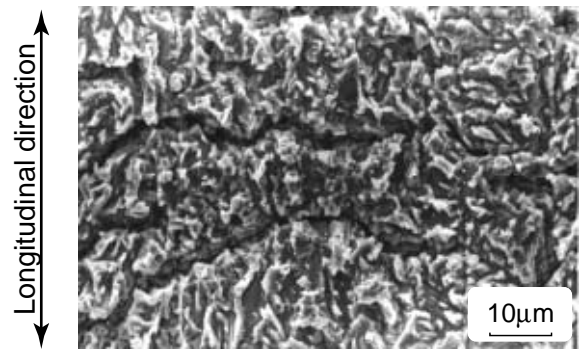


(a) Sample surface.

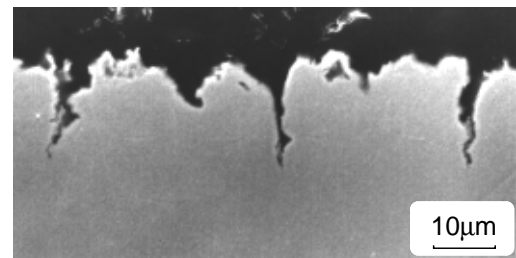


(b) Cross section along the longitudinal direction.

Figure 4: Corrosion fatigue damage at $\sigma_a = 167$ MPa ($\sigma_m = 115$ MPa, $N_f = 7.4 \times 10^6$)



(a) Sample surface.



(b) Cross section along the longitudinal direction.

Figure 5: Corrosion fatigue damage at $\sigma_a = 167$ MPa ($\sigma_m = 115$ MPa, $N_f = 1.2 \times 10^7$)

curves) of fatigue conducted in laboratory air and in NaCl solution. The superscript “*” denotes the number of cycles to failure of an interrupted fatigue test mentioned before. Although the number of samples conducted in laboratory air is small, fatigue strength in NaCl solution was almost equal to that conducted in laboratory air. The run-out result conducted at a stress amplitude of 50 MPa was that of a simulated test of a service stress condition. These indicate that the trolley wire is strong enough for fatigue loading of a service operation. In a corrosive environment, the crack which led the final failure was initiated not at the exposed surface, but at the coated surface. This indicates that the fatigue fracture mechanism operating in a corrosive environment was the same as that of the fatigue conducted in laboratory air. Note that the failed specimen at a stress amplitude of 167 MPa was fractured at a gripping position due to fretting, and this is considered an exception.

Corrosion fatigue damage

Figures 3 to 5 illustrate the SEM images of corrosion-fatigued specimen surface and the cross sections along

the loading direction. It is clear that the specimen surfaces were subjected to general corrosion, and no corrosion pit that would induce the crack initiation was observed. The morphology of the general corrosion was influenced by the texture of the material owing to drawing. The amount of general corrosion increased with an increase in the number of cycles (compare Fig. 5 with Fig. 3).

In order to investigate the influence of the varying load on general corrosion, interrupted tests were conducted in samples with and without cyclic loading, and the changes in surface were examined by atomic force microscopy. The results are shown in Fig. 6 (under varying loads) and Fig. 7 (without loading). The longitudinal grooves that were observed in the virgin samples were due to final finish by diamond paste. From these AFM images and SEM images that are not shown here, the corrosion preferentially progressed along the longitudinal direction. This may be resulted from the influence of the longitudinal scratches induced by polishing and the longitudinal textures due to drawing. The second important thing which could be deduced from the figures is that the corrosion morphology was not influenced by varying load when the crack was not nucleated on the surface. Figure 8 illustrates the changes in roughness, root mean square roughness (RMS) and center plane roughness, R_a , measured with the AFM. Note that the unit used is nm. It is clear that the both roughness increased with an increase in testing duration, and no influence of varying load was observed. This indicates that although the corrosion behavior of this material was dependent on the microstructure, no influence of varying load was observed, as far as severe plastic deformation did not occur. When the testing duration was larger than 25 h, the roughness became smaller. This is due to measurement error owing to large roughness. The principle of the operation of the AFM is that the small, sharp tip positioned at the end of a micromachined small, weak cantilever is raster-scanned on the surface: the observed surface was so rough that the tip could not reach the bottom of the surface.

Corrosion fatigue crack

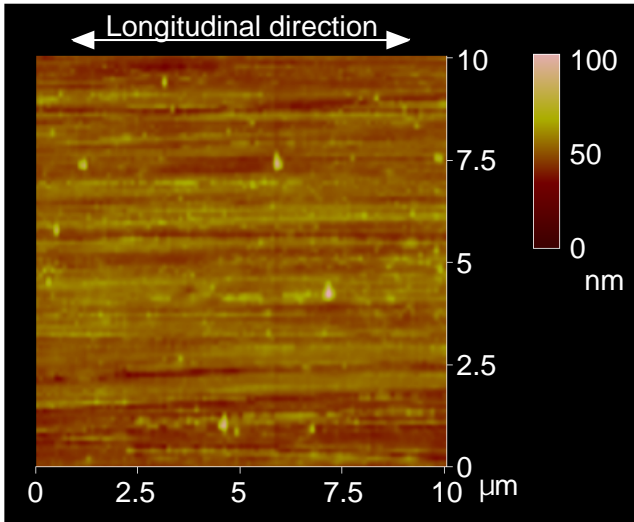
When the applied stress was high, multiple short transverse cracks were formed on the exposed surface (see Fig. 3(a)). Cross sectional views showed that the depth of these cracks remained short and was about 10 μm (Fig. 3(b)). The other noticeable point is that the crack wall was corroded, and this is in particular large near the surface. When the multiple cracks are formed on the surface, the stress concentration factors are increased or decreased depending on the distribution of surface defects. Ishida and Igawa [14] investigated the influence of multiple crack distribution on the stress intensity factor of a crack in a infinite body. They showed that the stress intensity factor is decreased when the cracks lined up, but increased when the cracks are distributed in a zigzag manner. From Fig. 3, the surface cracks tended to line up rather than to form in a zigzag manner. This indicates that the multiple crack formed on the surface may release the stress concentration, leading to lower crack growth rate.

As is discussed, multiple transverse cracks were nucleated, and then they grew due to coalescence (Figs. 4(a) and 5(a)). When multiple long cracks become long as shown in Fig. 5(a), the stress concentration factors are decreased. In addition, the crack walls were severely corroded, and the crack tip became blunt (Fig. 5(b)). From Fig. 4(b) and Fig. 5(b), it is clear that the extension of the crack toward the inside of the specimen was relatively short. The apparent crack growth rate computed was small, and was obtained at about $1.1 \times 10^{-11} \text{ m/s} \approx 5.5 \times 10^{-13} \text{ m/cycle}$. This was caused by the relief of the stress concentration due to crack blunting, and the crack growth rate became so much as that of general corrosion rate.

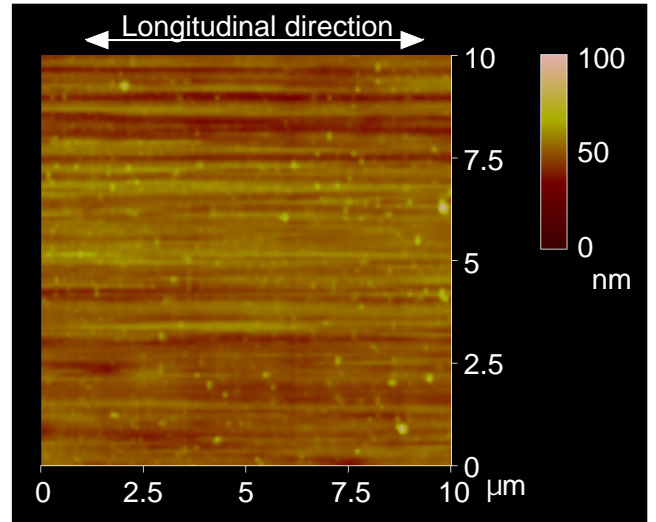
DISCUSSIONS

Corrosion fatigue mechanism can be summarized as follows [15]: in the case of a polycrystalline metallic material, the selective corrosion preferentially occurs at the deforming area, resulting in a corrosion pit. When the passive film or oxide film is formed, cyclic loading induces the breakage of the film owing to slip step formation, and the dissolution concentrates there. This may lead a corrosion pit initiation and progression. The corrosion fatigue crack is then initiated when the corrosion pit size, or depth, exceeds a critical value.

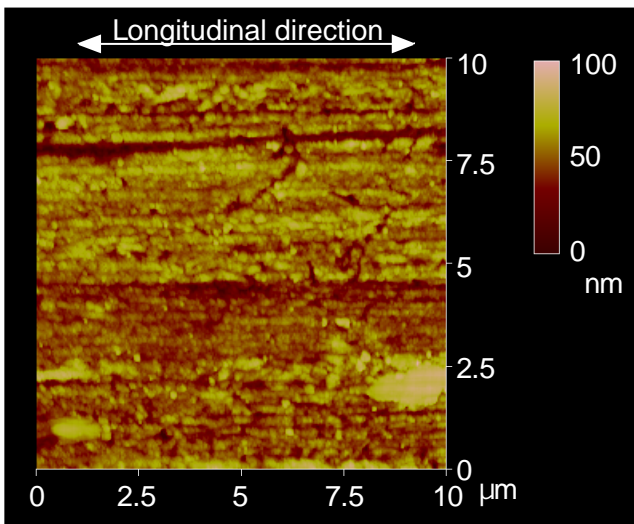
In the case of the Cu trolley wire tested here, however, the general corrosion prevailed on both cases of with and without cyclic loading, and the localized corrosion such as pitting did not occur. In the exposed area, multiple cracks were formed, and these yielded the relief of stress concentration. Severe general corrosion occurred, and this decreased the actual crack depth, and at the same time, caused crack tip blunting. These decreased the crack growth rate of both surface and depth directions. This is the reason why the final failure was brought about by the crack that was initiated at the anti-corrosive coated surface, where the mechanical factors dominated over the fracture, and the initiation and growth mechanism was the same as that of the fatigue in air. These may yield the speculation that when the entire part is exposed to a corrosive environment and a higher stress than the fatigue limit in air is applied, the corrosion fatigue strength would become higher than that in air. This is due to a decrease in corrosion fatigue crack growth rate. However, at a longer fatigue life region, i.e., larger than 1.0×10^8 cycles, the corrosion fatigue strength may be decreased from that conducted in



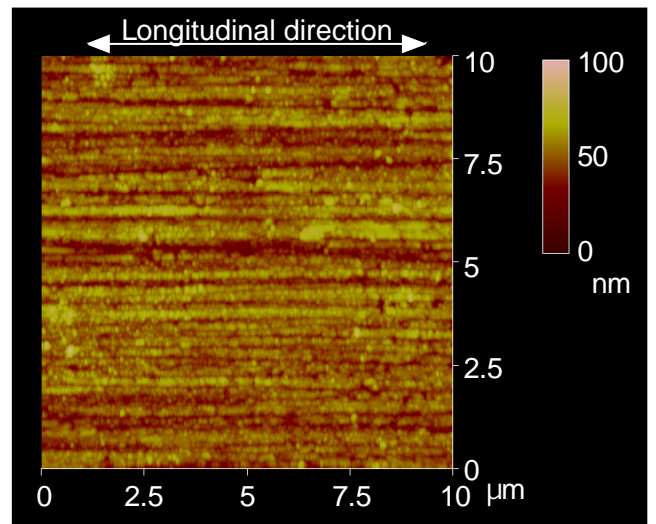
(a) Virgin sample surface



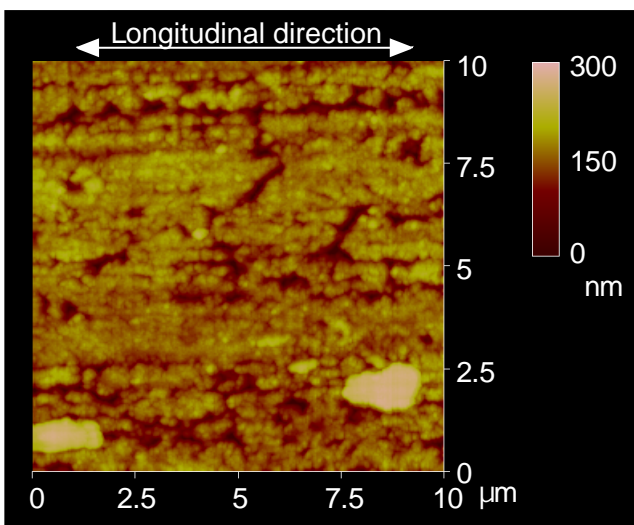
(a) Virgin sample surface



(b) $n = 1.4 \times 10^5$, corresponding to two hour testing.

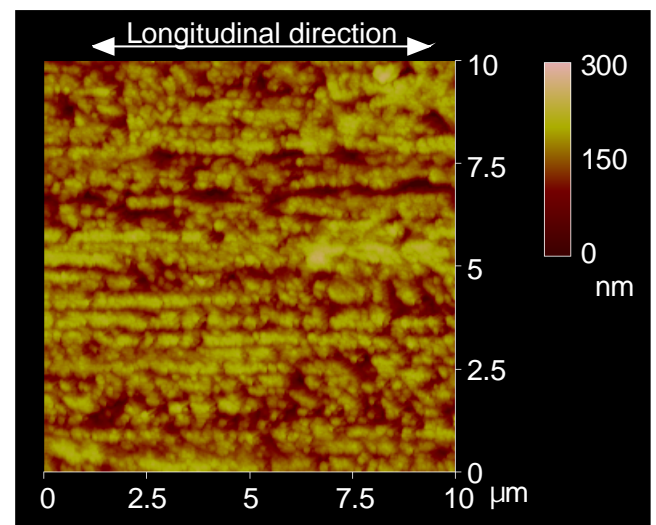


(b) Testing duration: two hours.



(c) $n = 7.2 \times 10^5$, corresponding to ten hour testing

Figure 6: AFM imaging of the sample surface fatigued at $\sigma_a = 196$ MPa with $\sigma_m = 115$ MPa in a 3.5% NaCl solution. The test was periodically interrupted to observe the sample surface.



(c) Testing duration: ten hours.

Figure 7: AFM imaging of the sample surface without any loading in a 3.5% NaCl solution (Static corrosion). The test was periodically interrupted to observe the sample surface.

air, because the severe general corrosion causes a decrease in diameter of the wire itself. The amount of a decrease in the wire diameter due to general corrosion can be estimated at 5 to 8 %/ year of the virgin wire diameter of 15 mm. In a service operation, however, the design stress is $\sigma_a = 50$ MPa, and therefore, a decrease in fatigue strength due to a loss of wire diameter by general corrosion is considered small. Hence, it is concluded that the newly developed Cu trolley wire has a enough fatigue strength for a service operation.

CONCLUSIONS

Fatigue tests were performed in a newly developed Cu trolley wire in laboratory air and in NaCl aqueous solution. The corrosion damage was closely examined with a scanning electron and atomic force microscopy. The investigation yielded the following conclusions:

1. The corrosion fatigue strength of the Cu trolley wire in a 3.5% NaCl solution is as much as strong as that in laboratory air: the wire has enough fatigue strength in a service operation.
2. The surface exposed to NaCl solution suffers from general corrosion, and no localized corrosion such as a corrosion pit, that may cause the corrosion fatigue crack initiation, exists. Note that the amount of general corrosion increases with an increase in exposure time.
3. No influence of cyclic loading on the morphology and the amount of general corrosion is observed even in the nanometer order, when the applied stress is low and the plastic deformation or slip remains small.
4. The corrosion fatigue strength in NaCl solution is determined by the fatigue strength in laboratory air: a decrease in stress concentration due to multiple cracks formed on the exposed surface, crack tip blunting due to dissolution of the crack wake, and a decrease in crack depth due to general corrosion cause a decrease in corrosion fatigue crack growth rate. The final failure is then brought about by the crack that is initiated on the coated surface, where no environmental influence exists.

ACKNOWLEDGMENT

The authors wish to express their thanks to Mr. S. Amagumo, Sumitomo Electric Co, Ltd., for the donation of the test materials.

REFERENCES

1. Komai, K., Minoshima, K., Kinoshita, S. and Kim, G. (1988), *JSME International Journal*, 31, 606.
2. Kondo, Y. (1987), *Trans. Japan Soc. Mech. Eng., Series A*, 53, 1983.
3. Nakajima, M., Kunieda H., Tokaji, K. (1991), *Trans. Japan Soc. Mech. Eng., Series A*, 57, 2859.
4. Komai, K., Minoshima, K., and Kim, G. (1988), *J. Soc. Mater. Sci., Japan*, 36, 141.
5. Minoshima, K., Nagashima, I., and Komai, K. (1998), *Fatigue & Fracture Eng. Mater. & Technology*, 21, 1435.
6. Komai, K., Minoshima, K., and Itoh, M. (1994), *J. Soc. Mater. Sci., Japan*, 43, 336.
7. Komai, K., Minoshima, K. and Miyawaki, T. (1998), *JSME International Journal, Series A*, 41, 49.
8. Ishii, H., Miyazu, S., Nakura, K. and Tohgo, K. (1993), *Trans. Japan Soc. Mech. Eng., Series A*, 59, 3014.
9. Sriram, T.S. Ke, C-M and Chung, Y. W. (1993), *Acta Metall.*, 41, 2515.
10. Harvey, S. E., Marsh, P. G. and Gerberich, W. W. (1994), *Acta Metall.*, 42, 3493.
11. Ikeda, K., Ito, S., Okada, T., Tenkumo, M., Yamamoto, M., Oku, G. and Maruyama, T. (1994), *Sumitomo Electric Review*, 145, 33.
12. Suto, H., Tamura, I. and Nisizawa, T. (1972), In: *Texture of Metallic Materials*, Maruzen Co. Ltd, Tokyo, Japan.
13. Nishida, M. (1973), In: *Stress Concentration*, Morikita Publishing Co., Ltd., Tokyo, Japan.
14. Isida, M. and Igawa, H. (1992), *Int. J. Fracture*, 53, 249.
15. Endo, K. and Komai, K. (1982), In: *Corrosion Fatigue of Metals and Strength Design*, Yokendo, Tokyo, Japan.

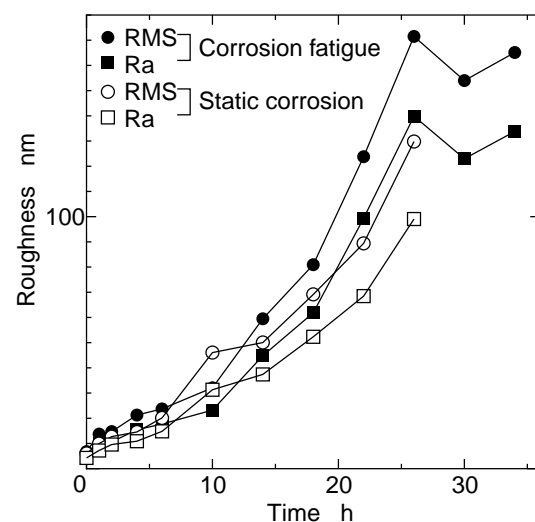


Figure 8: Changes in roughness of sample surface of corrosion fatigue and static immersion without loading.